Spectrochimica Acta Part A: Molecular and Biomolecular Spectroscopy 98 (2012) 329–336

Contents lists available at SciVerse ScienceDirect

Spectrochimica Acta Part A: Molecular and Biomolecular Spectroscopy

journal homepage: www.elsevier.com/locate/saa

The antibacterial activity of some sulfonamides and sulfonyl hydrazones, and 2D-QSAR study of a series of sulfonyl hydrazones

H. Güzin Aslan [a], Servet Özcan [b], Nurcan Karacan [c,*]

[a] Department of Chemistry, Science and Art Faculty, Erciyes University, 38039 Melikgazi, Kayseri, Turkey
[b] Department of Biology, Science and Art Faculty, Erciyes University, 38039 Melikgazi, Kayseri, Turkey
[c] Department of Chemistry, Science and Art Faculty, Gazi University, 06500 Ankara, Turkey

HIGHLIGHTS

- New original sulfonamide and sulfonyl hydrazones were synthesized.
- New compounds were screened for their antibacterial activity.
- 2D-QSAR analysis was performed on aromatic sulfonyl hydrazones used as antimicrobial agents against *Escherichia coli* and *Staphylococcus aureus*.

GRAPHICAL ABSTRACT

Plot of experimental versus predicted pMIC values of training sets of *Escherichia coli* and *Staphylococcus aureus*.

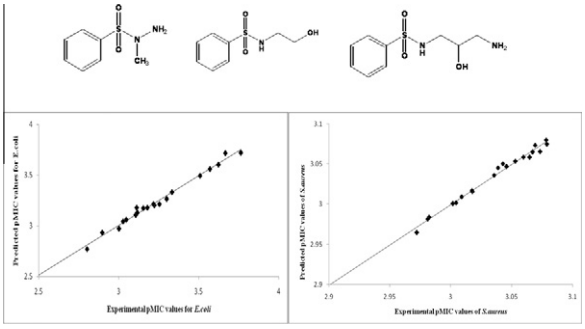

ARTICLE INFO

Article history:
Received 25 February 2012
Received in revised form 4 July 2012
Accepted 8 August 2012
Available online 1 September 2012

Keywords:
Sulfonamides
Sulfonyl hydrazones
Antibacterial activity
QSAR

ABSTRACT

Benzenesulfonicacid-1-methylhydrazide **(1)** and its four aromatic sulfonyl hydrazone derivatives (**1a–1d**), N-(3-amino-2-hydroxypropyl)benzene sulfonamide **(2)** and N-(2-hydroxyethyl)benzenesulfonamide **(3)** were synthesized and their structures were determined by IR, ^{1}H NMR, ^{13}C NMR, and LCMS techniques. Antibacterial activities of new synthesized compounds were evaluated against various bacteria strains by microdilution and disk diffusion methods. The experimental results show that presence of OH group on sulfonamides reduces the antimicrobial activity, and antimicrobial activities of the sulfonyl hydrazones **(1a–1d)** are smaller than that of the parent sulfonamide **(1)**, except *Candida albicans*. In addition, 2D-QSAR analysis was performed on 28 aromatic sulfonyl hydrazones as antimicrobial agents against *Escherichia coli* and *Staphylococcus aureus*. In the QSAR models, the most important descriptor is total point-charge component of the molecular dipole for *E. coli*, and partial negative surface area (PNSA-1) for *S. aureus*.

Introduction

Infectious diseases which increase dramatically by resistant and multiresistant microbes [1,2] are nowadays the second major cause of death worldwide and the third leading cause of death in developed countries [3,4]. Although the search for new lead structures for the development of antimicrobial agents is an increasingly important problem in medicinal chemistry. Pharmaceutical companies are leaving this area due to economic reasons [5]. It is well-known that sulfonamides and sulfonylhydrazones exhibit a broad spectrum of biological activities such as antimicrobial [6,7], antitumor [8], antidepressant-like activity [9] e.g., therefore,

* Corresponding author. Tel.: +90 312 2021117; fax: +90 312 2122279.
E-mail address: nkaracan@gazi.edu.tr (N. Karacan).

1386-1425/$ - see front matter © 2012 Elsevier B.V. All rights reserved.
http://dx.doi.org/10.1016/j.saa.2012.08.043

scientist have directed considerable attention on their synthesis, bioactivity and computational studies [10–12].

In our previous studies, sulfonic acid hydrazides and their hydrazones were obtained and screened for their antimicrobial and cytotoxic activity [13–17]. As part of our ongoing studies, new aromatic sulfonamides **(1–3)** and sulfonylhydrazone derivatives **(1a–1d)** were obtained and their structures were characterized by FT-IR, ^{1}H NMR, ^{13}C NMR and LC/MS techniques. Their antibacterial activities against Gram-positive (*Staphylococcus aureus* ATCC 25923, *Bacillus cereus* ATCC 11778, *Enterococcus faecalis* ATCC 29212, *Bacillus subtilis* ATCC 6633, *Staphylococcus epidermidis* ATCC 12228, *Enterobacter aerogenes* ATCC 13048) and Gram-negative bacteria (*Pseudomonas fluorescens* ATCC 49838, *Klebsiella pneumonia* ATCC 13883, *Escherichia coli* ATCC 25922, *Pseudomonas aeruginosa* ATCC 27853) and also antifungal activity against *Candida albicans* ATCC 90028 were screened by both microdilution and disk diffusion methods. In addition, 2D-QSAR studies were performed on a series of sulfonyl hydrazones, all of them synthesized previously by us, using the antimicrobial activity values (pMIC) of *E. coli* and *S. aureus* as dependent variables.

Experimental

The elemental analyses (C, H, N and S) were performed on a LECO-CHSNO-9320 type elemental analyzer. The IR spectra (4000–400 cm^{-1}) were recorded on a Mattson-1000 FT-IR spectrophotometer with samples prepared as KBr pellets. NMR spectra were recorded on a Bruker-Spectrospin Avance DPX-400 UltraShield (400 MHz) using *DMSO-d_6* and $CDC1_3$ as a solvent and TMS as an internal standard. LC/MS-APC1 were recorded on AGILENT 1100. The melting point was recorded on a Opti MELT 3 hot stage apparatus. TLC was conducted on 0.25 mm silica gel plates (60F254, Merck). Visualization was made with ultraviolet light. All extracted solvents (all from Merck) were dried over anhydrous Na_2SO_4 and evaporated with a BUCHI rotary evaporator. Reagents were obtained commercially from Aldrich (ACS grade) and used as received.

General procedure for the synthesis

Compounds **(1–3)** were synthesized by well-known substitution reactions between various amines and benzenesulfonyl chloride. Similarly, compounds **(1a–1d)** were obtained by substitution reactions between various aldehydes and compound **(1).** Structures of the sulfonamides **(1–3)** were shown in Fig. 1. Structural formula of the new sulfonyl hydrazones **(1a–1d)** were given in Table 1. Generally, THF solution of amines (or hydrazide) was added slowly drop by drop to the THF solution of benzenesulfonyl chloride (or aldehydes). In this process, temperature was kept between −5 and −10 °C, and the mixture was stirred for 24 h at room temperature. After the completion of the reaction (monitored by TLC), solvent was filtered in vacuum. The product was purified by column chromatography. The products were purified by silica gel 60 (230–400 mesh) column chromatography with THF as eluent.

*Benzenesulfonicacid-1-methylhydrazide (**1**)*

The general synthetic method described above was applied by using methylhydrazide (4.4 mL, 0.08 mol) and benzenesulfonyl chloride(5.05 mL, 0.04 mol). Yield 62%; mp 67–68 °C; MS (70 eV, APC1): 186.1 (M^+, 100%), 185.1, ($M-H^+$, 11.5%), 171.1($M-CH_3^+$, 10.5%), 142.1($M-C_6H_5SO_2^+$, 10.5%); Anal. Calcd for $C_7H_{10}N_2O_2S$: C, 45.09; H, 5.43; N, 15.09; S, 17.19. Found: C, 45.14; H, 5.41; N, 15.04; S, 17.21.

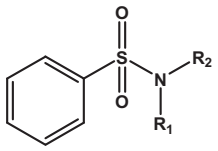

(1) R_1= NH_2, R_2= CH_3
(2) R_1=H, R_2= CH_2CH_2OH
(3) R_1=H, R_2=$CH_2CH(OH)CH_2NH_2$

Fig. 1. Structures of the sulfonamides.

*N-(3-amino-2- hydroxypropyl)benzenesulfonamide (**2**)*

The general synthetic method described above was applied by using benzenesulfonyl chloride (5.05 mL, 0.04 mol) and 1,3-diamino-2-propanol (7.21 g, 0.08 mol). Yield 51%; mp 155 °C; MS (70 eV, APC1): 231.26 ($M+H^+$, 100%), 231.2($M-C_6H_5SO_2H_2^+-$, 13.1%), Anal. Calcd for $C_9H_{14}N_2O_3S$:C, 47.00; H, .13; N, 12.10; S, 13.91. Found: C, 46.94; H, 6.12; N, 12.16; S, 13.92.

*N-(2-hydroxyethyl)benzenesulfonamide (**3**)*

The general synthetic method described above was applied by using benzenesulfonyl chloride (5.05 mL, 0.04 mmole) and ethanolamine(4.83 mL, 0.08 mol). Yield 65%; mp 79–80 °C; MS (70 eV, APC1): 200.3 ($M-H^+$–, 100%), 214.1($M+NH_4^+$, 13.2%), Anal. Calcd for $C_8H_{11}NO_2S$: C, 47.70; H, 5.61; N, 7.00; S, 15.83. Found: C, 47.74; H, 5.52; N, 6.96; S, 15.93.

*Salicylaldehydebenzenesulfonylhydrazone (**1a**)*

The general synthetic method described above was applied by using yellow solid **(1)** (3.1 mL, 46.0 mmole) and salicylaldehyde (3 mL, 23.0 mmole). The product was crystallized from ethanol/hexane mixture (3:1). Yield 82%; mp 112–113 °C; MS (70 eV, APC1): 301.1 ($M+l^+$, 62.8%), 302.1 ($M+2^+$, 9.0%), 303.1 ($M+3^+$, 7.1%), 134.1 ($M-2^+-C_3H_7SO_2NH(CH_2)_2$, 21.7%), 164.1 ($M^+-C_4H_9SO_2NH$, 37.9%); Anal. Calcd for $C_{10}H_{24}N_2O_4S_2$: C, 40.0; H, 8.0; N, 9.33.; S, 21.3. Found: C, 40.23; H, 7.94; N, 9.10; 8, 21.51.

*2-hydroxy-1-acetophenonbenzenesulfonylhydrazone (**1b**)*

The general synthetic method described above was applied by using yellow solid **(1)** (3.95 mL, 47.5 mmole) and 1-hydroxyacetophenon (3.0 mL, 23.7 mmole). The product was crystallized from ethanol/hexane mixture (2:1). Yield 88%; mp 116–117 °C; MS (70 eV, APC1): 315.1 ($M+l^+$–, 100%), 316.1 ($M+2^+$–, 14.5%), 317.1 ($M+3^+$, 10.4%), 195.1 ($M+2^{+\prime}-C_4H_9SO_2$–, 31.5%); Anal. Calcd for $CnH_{26}N_2O_4S_2$: C, 42.04; H, 8.28; N, 8.92; S, 20.38. Found: C, 42.17; H, 8.45; N, 9.32; S, 19.98.

*2-hydroxy-1-naphtaldehydebenzenesulfonylhydrazone (**1c**)*

The general synthetic method described above was applied by using yellow solid **(1)** (4.7 mL, 47.4 mmole) and 2-hydroxynaftaldehyde (3.0 mL, 23.7 mmole). Product was recrystallized from ethanol/benzene mixture (2:1). Yield 88%; mp 117–118 °C; MS (70 eV, APC1): 329.1 ($M+1^+$, 100%), 330.1($M+2^+$, 16.1%), 331.1 ($M+3^+$, 11.1%), 209.1 ($M+2^{+1}-C_4H_9SO_2$, 28.9%), 192.1 ($M^+-C_4H_9SO_2NH$, 9.2%); Anal. Calcd for $C_{12}H_{28}N_2O_4S_2$: C, 43.9; H, 8.5; N, 8.5; S, 19.5. Found: C, 44.33; H, 8.37; N, 8.61; S, 19.52.

*Thiophene-2-carbaldehyde benzenesulfonylhydrazone (**1d**)*

The general synthetic method described above was applied by using yellow solid **(1)** (2.0 mL, 16.0 mmole) and thiophene-2-carbaldehyde (1.06 mL, 8.1 mmole). The product was crystallized from methanol/hexane mixture (2:1). Yield 80%; mp 123–124 °C; MS (70 eV, APC1): 343.5 ($M+1^+$, 100%), 344.15 ($M+2^+$, 16.1%), 345.1 ($M+3^+$, 10.1%), 223.1 ($M+2^+-C_4H_9SO_2$, 3.9%); Anal. Calcd for $C_{13}H_{30}$-

Table 1
Structural formula and observed pMIC values for the studied data sets of 28 aromatic sulfonyl hydrazones.

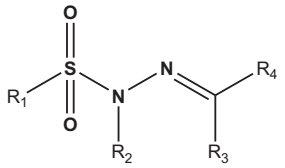

. Compounds	R_1	R_2	R_3	R_4	EC[a](pMIC)	SA[b](pMIC)
(1a)	$-C_6H_5$	$-CH_3$	—H	—2-OH—C_6H_4	2.8978	2.9722
(1b)	$-C_6H_5$	$-CH_3$	$-CH_3$	—2-OH—C_6H_4	2.8012	2.9824
(1c)	$-C_6H_5$	$-CH_3$	—H	—2-OH—$C_{10}H_6$	3.5550	2.9708
(1d)	$-C_6H_5$	$-CH_3$	—H	$-C_4H_3S$	3.3327	2.9812
SALMSH	$-CH_3$	—H	—H	—2-OH—C_6H_4	3.1062	3.0673
SALESH	$-CH_2CH_3$	—H	—H	—2-OH—C_6H_4	3.2016	3.0685
SALPSH	$-CH_2CH_2CH_3$	—H	—H	—2-OH—C_6H_4	3.1128	3.0784
AFMSH	$-CH_3$	—H	$-CH_3$	—2-OH—C_6H_4	3.1540	3.0532
AFESH	$-CH_2CH_3$	—H	$-CH_3$	—2-OH—C_6H_4	3.3008	3.0571
AFPSH	$-CH_2CH_2CH_3$	—H	$-CH_3$	—2-OH—C_6H_4	3.2538	3.0693
NAFMSH	$-CH_3$	—H	—H	—2-OH—$C_{10}H_6$	3.1790	3.0734
NAFESH	$-CH_2CH_3$	—H	—H	—2-OH—$C_{10}H_6$	3.2343	3.0373
NAFPSH	$-CH_2CH_2CH_3$	—H	—H	—2-OH—$C_{10}H_6$	3.2227	3.0357
SALMSMH	$-CH_3$	$-CH_3$	—H	—2-OH—C_6H_4	3.2993	3.0460
SALESMH	$-CH_2CH_3$	$-CH_3$	—H	—2-OH—C_6H_4	3.0427	3.0548
SALPSMH	$-CH_2CH_2CH_3$	$-CH_3$	—H	—2-OH—C_6H_4	3.2159	3.0597
AFMSMH	$-CH_3$	$-CH_3$	$-CH_3$	—2-OH—C_6H_4	3.5078	3.0019
AFESMH	$-CH_2CH_3$	$-CH_3$	$-CH_3$	—2-OH—C_6H_4	3.5584	3.0095
AFPSMH	$-CH_2CH_2CH_3$	$-CH_3$	$-CH_3$	—2-OH—C_6H_4	3.5686	3.0090
NAFMSMH	$-CH_3$	$-CH_3$	—H	—2-OH—$C_{10}H_6$	3.0466	3.0429
NAFESMH	$-CH_2CH_3$	$-CH_3$	—H	—2-OH—$C_{10}H_6$	3.1526	3.0603
NAFPSMH	$-CH_2CH_2CH_3$	$-CH_3$	—H	—2-OH—$C_{10}H_6$	3.1162	3.0389
5MSALMSH	$-CH_3$	—H	—H	—2-OH—5-Me—C_6H_3	3.0018	3.0649
5MSALESH	$-CH_2CH_3$	—H	—H	—2-OH—5-Me—C_6H_3	3.1040	3.0778
5MSALPSH	$-CH_2CH_2CH_3$	—H	—H	—2-OH—5-Me—C_6H_3	3.0278	3.0791
5MAFMSH	$-CH_3$	—H	$-CH_3$	—2-OH—5-Me—C_6H_3	3.6226	3.0044
5MAFESH	$-CH_2CH_3$	—H	$-CH_3$	—2-OH—5-Me—C_6H_3	3.7633	3.0179
5MAFPSH	$-CH_2CH_2CH_3$	—H	$-CH_3$	—2-OH—5-Me—C_6H_3	3.6659	3.0175

[a] *E. coli* ATCC 25922.
[b] *S. aureus* ATCC 25923.

$N_2O_4S_2$: C, 45.6; H, 8.77; N, 8.18; S, 18.71. Found: C, 45.87; H, 8.20; N, 8.16; S, 18.94.

Biological activity: in vitro evaluation

Biological activity of the synthesized compounds were individually screened against a panel of microorganisms, including Gram-positive (*S. aureus* ATCC 25923, *B. cereus* ATCC 11778, *E. faecalis* ATCC 29212, *Bacillus subtilis* ATCC 6633, *S. epidermidis* ATCC 12228, *E. aerogenes* ATCC 13048), Gram-negative bacteria (*P. fluorescens* ATCC 49838, *K. pneumonia* ATCC 13883, *E. coli* ATCC 25922, *P. aeruginosa* ATCC 27853) and yeast (*C. albicans* ATCC 90028). Cultures were obtained from Erciyes University, Department of Biology. Bacterial strains were cultured overnight at 35 °C in Triptic Soy Broth (TSB) and the yeast was cultured overnight at 30 °C in Yeast-extract Peptone Dextrose Broth (YPDB) in a rotary shaker at 200 rpm. Overnight cultures were then transferred to fresh medium and adjusted the turbidity of all broth cultures to 0.1 absorbance at 640 nm on a spectrophotometer. These stock cultures were stored in the dark at 4 °C during the survey.

Microdilution method

Minimal inhibitory concentrations (MIC) were determined by microdilution broth method following the procedures recommended by the National Committee for Clinical Laboratory Standards (NCCLSs, 2000) [18]. Shortly, synthesized compounds dissolved in dimethylsulfoxide (DMSO) were first diluted to the highest concentration, and then serial twofold dilutions were made in a concentration range from 31.25 to 2000 μg/mL in sterile 2.4 mL 96 well Masterblock dish containing either MHB for bacterial strains and or YPDB for the yeast. For the test, the 96-well plates were prepared by dispensing into each well 195 μL of serial dilutions of synthesized compounds was transferred into seven consecutive wells in each column. The last well, containing only 195 μL of MHB or YPDB without compound was used as negative control. For each columns of the plate, 5 μL of the strains to be tested inoculated to each well individually. The final volume in each well was brought to 200 μL by adding MHB or YPDB solution. For the bacterial cells; ampicilin, trymethoprim, tetracycline in MHB and for yeast miconazole and nystatin in YPDB at the concentration range of 1000–7.8 μg/mL was used as standard drug for positive control. Contents of each well were mixed on a plate shaker at 300 rpm for 20 s and then incubated at 35 °C for 18–24 h. Microbial growth was determined by absorbance at 600 nm using the Tecan Sunrise microplate reader and with the presence of a white "pellet" on the well bottom by visual examination. The concentration resulted with no growth confirmed by plating 5 μL samples from clear wells on MHA or YPDA. Every experiment in the antibacterial assay was replicated twice against each organism. MIC's were defined as the lowest concentrations of the antimicrobial agents that inhibited visible growth of the microorganism.

Disk diffusion method

Antibacterial screening of synthesized compounds dissolved in DMSO were performed using Miller Hinton Agar (MHA) for the bacterial strains and Yeast-extract Peptone Dextrose Agar (YPDA) for yeast cells. 100 μL of the culture suspensions adjusted to the OD_{640} 0.1 (equivalent to 0.5 Mc Farland Turbidity Tubes) were

Table 2
Four-parameter QSAR models by BMLR method.

	X	$\pm\Delta X$	t-Test	Descriptors
For E. coli				
Training set				
	R^2 = 0.9887	F = 327.0753	s^2 = 0.0010	R^2_{cv} = 0.9745
0	1.1619e−03	5.9281e−05	3.5999	Intercept
1	8.4052e−01	2.1365e−01	−25.2993	Tot point-charge comp. of the mol. dipole
2	7.5577e−01	6.4655e−01	11.6893	HOMO energy
3	6.2884e−01	1.4002e−01	5.9193	Relative number of aromatic bonds
4	8.4501e−03	3.8829e−03	−2.1762	Relative negative charged SA (RNCS)
Test set				
R^2 = 0.9644, RMSE = 0.0348				
For S. aureus				
Training set				
	R^2 = 0.9873	F = 290.3714	s^2 = 0.0001	R^2_{cv} = 0.9741
0	3.2572e−05	1.3049e−07	2.6141	Intercept
1	2.1309e+01	4.3953e−03	−25.7306	Partial negative surface area (PNSA-1)
2	1.1269e+01	2.4389e−01	−8.7205	Max nucleoph. react. index for a N atom
3	2.0901e−03	5.7156e−05	3.6568	H-acceptors surface area (HASA)
4	2.0286e−02	8.9030e−04	−2.2786	Relative number of double bonds
Test set				
R^2 = 0.9856, RMSE = 0.0048				

swabbed over the entire surface of the medium [19,20]. Sterile 6-mm-diameter disks (1.2 mm thickness whatman filter paper) were impregnated with 50 μL dissolved extracts (including 1.2 mg total extract per disk) placed onto MHA or YPDA. Negative controls were prepared just by using DMSO. For bacterial cells; ampicilin (50 μg/disk), trymethoprim (30 μg/disk), tetracycline (30 μg/disk) on MHA and for yeast miconazole (40 μg/disk) and nystatin (30 μg/disk) on YPDB were used as reference standards to determine the sensitivity of each strain. The inoculated plates were incubated at 35 °C for 18–24 h. The antibacterial activity was measured as the diameter (mm) of clear zone of growth inhibition. Four disks per plate and each test were run in duplicates.

QSAR analysis

Data sets

Antimicrobial activity values of a series of sulfonyl hydrazones, all of which synthesized in our laboratory previously [13–17,21–31], were screened against *S. aureus* ATCC 25923 and *E. coli*. Experimental MIC values were first transformed to pMIC (−logMIC) on a molar basis (listed in Table 1) and used as dependent variables to obtain the linear relationship. Twenty-eight data set was randomly separated into a training set of 20 compounds and a test set (prediction set) of eight compounds.

Descriptor calculation

Energy minimization of all of the compounds was performed by using Gaussian 03 software and semi-empirical AM1 method [32]. Gaussian outputs were loaded into the CODESSA (version 2.7.10) software to calculate more than 500 molecular descriptors (constitutional, topological, geometrical, electrostatic, quantum-chemical and thermodynamical descriptors). Online AlogPS 2.1 applet was used to calculate the log*P* values of our compounds [33]. Hydration energy values were calculated using HyperChem 7.5 software [34]. The "breaking point" rule was applied to determine the optimal number of descriptors in the model equations. This rule is based on the significant improvement of R^2 (ΔR^2 < 0.02–0.04) with respect to the number of descriptors in the model. Consequently, four descriptors were used as independent variables in our models (Table 2). The absence of colinearity among the used descriptors is confirmed by intercorrelation matrix for the independent variables in our models (Table 3). No significant correlation was found among the descriptors applied in the same equation; in fact, BMLR method in CODESSA softwere rejects descriptors with intercorrelation coefficients larger than a default (0.8) threshold value.

Regression analysis

Best Multiple Linear Regression (BMLR) method embedded in CODESSA software was used to obtain the QSAR models [35]. The BMLR regression algorithm generates the best n-parameter regression equation ($n \geqslant 2$), based on the highest R^2 and F values obtained in the process. During the calculation the decriptor scales are normalized and centered automatically. If the variables are mutually intercorrelated, the BMLR rejects descriptors with intercorrelation coefficients larger than a certain threshold value [36]. To validate the predictive capability of the models, the squared correlation coefficient (R^2), leave-one-out cross-validated squared correlation coefficient (R^2_{cv}), the Fisher criteria (F), and standard error (s^2) were used [37] for internal validation. High R^2 values (>0.9), small standard deviations (<0.07), high F values and high cross-validated squared correlation coefficient (>0.9) indicate the robustness of generated models. In order to check the performance of the obtained models (shown in Table 2), we apply the obtained linear model to the test set. R^2 was used to evaluate the fitness ability, and RMSE (root mean square error) was used to evaluate the predictive capability of the model. The statistical parameters for the test sets were R^2 = 0.9644 and RMSE = 0.0348 for *E. coli*, R^2 = 0.9856 and RMSE = 0.0048 for *S. aureus*, confirming the capability of the model derived from the training set.

Results and discussion

Structure of the compounds

Experimental ^{1}H and ^{13}C NMR chemical shift values of our compounds were listed in Table 4. Proton chemical shift values of **(1)** and **(2)** were reported previously, but we have found no reference about their carbon atom chemical shift values in the literature [38,39]. Carbon atom peaks of the compounds were assigned using theoretical chemical shift values calculated with GIAO/DFT/B3LYP/++6-311G(2d,2p) methods in DMSO solution. In the NMR spectra of the compounds, proton signals of aromatic moiety appear at 6.90–8.12 ppm, and aromatic carbon peaks appear at 164.01 and

Table 3
Correlation matrix of the descriptors involving in the QSAR models.

	For *E. coli*					For *S. aureus*			
	HOMO	RNAO[a]	RNCS[b]	TPC[c]		RNDB[d]	MNRI[e]	PNSA-1[f]	HASA[g]
HOMO	1.0000				RNDB	1.0000			
RNAO	0.6112	1.0000			MNRI	−0.0570	1.0000		
RNCS	0.3162	0.2377	1.0000		PNSA-1	−0.4512	0.2644	1.0000	
TPC	−0.1244	0.1154	−0.2046	1.0000	HASA	0.2532	−0.6185	−0.0410	1.0000

[a] RNAO: Relative number of aromatic bonds.
[b] RNCS: Relative negative charged SA.
[c] TPC: Tot point-charge comp. of the molecular dipole.
[d] RNDB : Relative number of double bonds.
[e] MNRI: Max nucleoph. react. index for a N atom.
[f] PNSA-1: Partial negative surface area.
[g] HASA: H-acceptors surface area.

Table 4
The ^{1}H and ^{13}C NMR chemical shifts values in d_6-DMSO (ppm) of the new compounds.

Assignments	(**1a**)	(**1b**)	(**1c**)	(**1d**)	(**1**)	(**2**)	(**3**)
^{1}H NMR data							
C—C**H$_3$**	–	2.30(s,3H)	–	–	–	–	–
N—C**H$_3$**	2.60(s,3H)	2.61(s,3H)	2.60(s,3H)	2.97(s,3H)	3.31(s,3H)	–	–
NH$_2$	–	–	–	–	3.81(s,2H)	–	n.o.
N**H**	–	–	–	–	–	8.44(br)	7.15(br)
C**H$_2$**(a)	–	–	–	–	–	2.83(t,2H)	2.88(d,2H)
C**H$_2$**(b)	–	–	–	–	–	3.59(t,2H)	2.66(d,2H)
C**H**(c)	–	–	–	–	–	–	3.87(s,1H)
N=C**H**	8.60(s,1H)		9.98(s,1H)	8.73(s,1H)	–	–	–
O**H**	10.31(s,1H)	12.93(s,1H)	12.85(s,1H)	–	–	5.18(s,1H)	7.15 (br)
Ar**H**	6.90–7.58	7.43–6.97	8.05–7.31	7.19–8.43	8.12–7.63	8.44(br)	6.51–7.30
^{13}C NMR data							
C—**C**H$_3$	–	15.55	–	–	–	–	–
N—**C**H$_3$	35.22	36.97	37.01	37.02	40.46	–	–
CH$_2$(a)	–	–	–	–	–	45.42	42.47
CH$_2$(b)	–	–	–	–	–	60.08	40.59
CH(c)	–	–	–	–	–	–	64.87
N=**C**H	141.61	133.60	161.10	156.02	–	–	–
Ar**C**	158.22 –117.13	130.45 –119.81	164.01 –112.25	144.09 –122.11	148.13 –125.95	134.10 –125.77	129.07 –128.04

117.13 ppm. In the ^{1}H NMR spectra of (**2**) and **(3)**, a very broad band at ~8.4 ppm and ~7.4 ppm are assigned to overlapped NH, OH and aromatic proton peaks, respectively.

IR spectra Characteristic vibration of the compounds were summarized in Table 5. Asymmetric and symmetric NH_2 stretching vibrations of **(1)** were observed between 3140 and 3100 cm^{-1}. **(1)** is a very hydroscopic compound, existence of hydrogen bonding shifted its stretching vibrations towards lower wave numbers than we expected. The vibration observed at ~1608 cm^{-1} of **(3)** is assigned to $\Delta(NH_2)$ in-plane bending vibration. Secondary alcohol stretching vibration of **(3)** was shown at 1113 cm^{-1}. Terminal methyl group stretching vibrations of **(1)** were found at ~2974 cm^{-1}.

Antimicrobial activity

The synthesized compounds and reference drugs (tetracycline, trymethoprim, miconazole and nystatin) were screened *in vitro* against various pathogens. Their minimum inhibitory concentrations (MICs) were given in Table 6, and diameter of the inhibition zones (mm) were tabulated in Table 7. As seen in Table 3, the compound **(1)** is the most potent sulfonamide among this series.

Table 5
Wave numbers (cm^{-1}) of selected vibration bands of the new compounds.

Compounds	$\nu_{as}(NH_2)$[a]	$\nu_{s}(NH_2)$[b]	$\nu(NH)$[c]	$\Delta(NH_2)$[d]	$\nu_{as}(SO_2)$	$\nu_{s}(SO_2)$	$\Delta(SO_2)$	$\nu(CN)$	$\nu(CO)$
(**1**)	3141	3100	–	1600	1249	1157			
(**2**)	–	–	3290	–	1361	1151	501		
(**3**)	3360	3331	n.o[e]	n.o	1334	1156	525	–	–
(**1a**)	–	–	–	–	1295	1180	561	1659	1258
(**1b**)	–	–	–	–	1329	1150	517	1606	1271
(**1c**)	–	–	–	–	1344	1162	531	1636	1265
(**1d**)	–	–	–	–	1316	1166	520	1617	–

[a] υ_{as}: asymmetric stretching.
[b] υ_{s}: symmetric stretching.
[c] υ: stretching.
[d] Δ: bending.
[e] n.o: not observed.

Table 6
Antimicrobial activity of the new compounds with microdilution method (μg/mL).

	Pf[a]	*Pa*[b]	*Ec*[c]	*Kp*[d]	*Ea*[e]	*Sa*[f]	*Bc*[g]	*Bs*[h]	*Se*[i]	*Ef*[j]	*Ca*[k]
(**1**)	62.5	62.5	125	125	125	125	125	125	125	250	>2000
(**2**)	1000	1000	1000	>2000	1000	>2000	>2000	>2000	>2000	>2000	1000
(**3**)	1000	1000	1000	1000	1000	>2000	>2000	1000	>2000	>2000	1000
(**1a**)	500	1000	500	1000	1000	250	500	500	250	500	500
(**1b**)	1000	1000	1000	1000	1000	500	500	500	500	1000	500
(**1c**)	250	250	500	250	500	500	500	250	250	500	1000	500
(**1d**)	125	125	125	125	250	250	250	125	125	500	1000

[a] *P. fluorescens* ATCC 49838.
[b] P. *aeruginosa* ATCC 27853.
[c] *E. coli* ATCC 25922.
[d] *K. pneumonia* ATCC 13883.
[e] *E. aerogenes* ATCC 13048.
[f] *S. aureus* ATCC 25923.
[g] *B. cereus* ATCC 11778.
[h] *B. subtilis* ATCC 6633.
[i] *S. epidermidis* ATCC 2228.
[j] *E. faecalis* ATCC 29212.
[k] *C. albicans* ATCC 90028.

It showed good antibacterial activity against both Gram-negative bacteria (*P. fluorescens* at 62.5 μg/mL, *K. pneumonia* at 125 μg/mL, *E. coli* at 125 μg/mL, *P. aeruginosa* at 62.5 μg/mL) and Gram-positive bacteria (*S. aureus* 125 μg/mL, *B. Cereus 125* μg/mL, *E. faecalis* 250 μg/mL, *B. subtilis 125* μg/mL, *S. epidermidis* 125 μg/mL, *E. aerogenes 125* μg/mL), and also antifungal activity against *C. albicans* at >2000 μg/mL. In sulfonyl hydrazone series, compound **(1d)** showed observable activity against Gram-negative bacteria (*P. fluorescens* at *125* μg/mL, *K. pneumonia* at 125 μg/mL, *E. coli at 125* μg/mL, *P. aeruginosa* at 125 μg/mL) and Gram-positive bacteria (*B. subtilis 125* μg/mL, *S. epidermidis* 125 μg/mL).

Structure–activity relationships

Sulfonamide **(1)** showed good activity against Gram-negative bacteria, however, its sulfonyl hydrazones (**1a–1d)** showed moderate activity against both Gram-positive bacteria except *C. albicans*. According to disk diffusion data, reference drugs showed better activity than our compounds in all tested strains. Antimicrobial activities of the sulfonamides bearing hydroxyl group **(2–3)** were remarkably lower than that of **(1)**. It may be attributed that an increase in hydrophilicity of the sulfonamides would cause their antimicrobial activity to decrease. As seen in Table 8, log*P* values (0.34, −0.44, −1.03) and hydration energy values (−7.92, −12.81, −13.89 kcal/mol) of three sulfonamides **(1–3)** decrease as their activity decreases.

Thiophene ring-containing sulfonyl hydrazone **(1d)** showed the best antimicrobial activity against microorganism, however, the compound **(1d)** was found to be inactive against *C. albicans.* This result is perhaps not surprising as thiophene ring skeleton is widely found in many biologically active compounds [40], for example, Biotin (Vitamin H) is a tetrahydrothiophene. Naphthalene-containing sulfonyl hydrazones **(1c)** showed the second best antimicrobial activity. It is known that naphthalene groups can form cation–pi interaction and aromatic pi-stacking. When electron rich naphthalene encounters a cation or a positively charged group on protein, receptor site bonds the aromatic ring to make charge-transfer complex. This feature corresponds to some parameter such as RNABs (Relative number of aromatic bonds), RNBRs (Relative number of benzene rings), MPPBO (Max pi–pi bond order) (Table 8). As seen in Table 5, these parameters correlate with antibacterial activities of our compounds. However, to find a quantitative structure activity relationship, we need to perform statistical analysis. For this reason, a set of analog sulfonyl hydrazones, all of them synthesized earlier by us, were taken to perform the 2D-QSAR analysis.

QSAR analysis

Structures of 28 sulfonyl hydrazones and their antimicrobial activity against *E. coli* ATCC 25922 and *S. aureus* ATCC 25923 were listed in Table 1. In Table 2, four-parameter models obtained by using BMLR method are given in decreasing relevance order according to their statistical significance (ordered by *t*-test value). In these tables, X and ΔX are regression coefficients of the QSAR equation and their standard errors, respectively. A graphical presentation of the relationship between the experimental and the predicted pMIC values for training sets are given in Fig. 2.

In the QSAR model for *E. coli*, the most important descriptor is total point-charge component of the molecular dipole. This is an electrostatic descriptor and related with charge and polarizability. It presumably contributes general electrostatic interactions. Its positive coefficient indicates that activity of the compounds increases when the charge is distributed throughout the molecule. The second important descriptor is HOMO energy. HOMO energy level describes global and local nucleohilicity in cases of non-covalent molecular interactions. In general, a high-lying HOMO molecular orbital assumes a charge or electron transfer from the compound to the receptor. The third descriptor, relative number of aromatic bonds, is defined as the ratio of the number of aromatic bonds to the total number of bonds. The fourth descriptor is relative negative charged surface area (RNCS). It is an electrostatic descriptor and it deals with the features responsible for polar interactions between molecules. This descriptor is sensitive to both the size and the charge of the molecule.

In the QSAR model for *S. aureus,* the most important descriptor is partial negative surface area (PNSA-1). It is responsible for polar interactions between molecules. The larger value of the descriptor indicates the higher polarity of the molecule. The positive regression coefficient for this descriptor reflects the fact that the larger value of this descriptor leads to higher binding ability. The second important descriptor is maximum nucleophilic reactivity index for a N atom, which describes the tendency of a molecule to act as an nucleophile in a chemical reaction, in other words, it is related to electron transfer between the donor and the acceptor. Due to the positive sign of the regression coefficient, the higher the descriptor value is, (the molecule will act as a stronger nucleophile) the higher its antimicrobial effect will be. The third descriptor is H-acceptors surface area (HASA). It is related with hydrogen bond

Table 7
Antimicrobial activity of the new compounds (150 μg/disk) with disk diffusion method.

	Pf[a]	*Pa*[b]	*Ec*[c]	*Kp*[d]	*Ea*[e]	*Sa*[f]	*Bc*[g]	*Bs*[h]	*Se*[i]	*Ef*[j]	*Ca*[k]
(**1**)	22	19	18	17	16	19	15	16	14	15	0
(**2**)	0	0	0	0	0	0	0	0	0	0	0
(**3**)	0	0	0	0	0	0	0	0	0	0	0
(**1a**)	12	6	13	6	6	13	11	9	14	11	14
(**1b**)	11	5	11	6	5	10	10	9	12	9	12
(**1c**)	26	25	17	23	18	19	26	28	16	17	16
(**1d**)	25	24	17	21	17	12	25	24	15	0	0
Tetracycline (30 μg)	19	23	23	12	0	0	19	26	19	0	0
Trymethoprim (30 μg)	0	31	0	0	28	37	0	20	29	27	0
Miconazole (30 μg)	0	0	0	0	0	0	0	0	0	0	26
Nystatin (40 μg)	0	0	0	0	0	0	0	0	0	0	18

[a] *P. fluorescens* ATCC 49838.
[b] *P. aeruginosa* ATCC 27853.
[c] *E. coli* ATCC 25922.
[d] *K. pneumonia* ATCC 13883.
[e] *E. aerogenes* ATCC 13048.
[f] *S. aureus* ATCC 25923.
[g] *B. cereus* ATCC 11778.
[h] *B. subtilis* ATCC 6633.
[i] *S. epidermidis* ATCC 12228.
[j] *E. faecalis* ATCC 29212.
[k] *C. albicans* ATCC 90028.

Table 8
Some physicochemical properties of the new compounds.

	(**1**)	(**2**)	(**3**)	(**1a**)	(**1b**)	(**1c**)	(**1d**)
ALOGPs[a]	0.34	−0.44	−1.03	2.19	2.33	3.31	2.23
ΔH_h[b]	−7.92	−12.81	−13.89	−11.07	−8.83	−9.42	−6.60
RNAB[c]	0.27	0.25	0.21	0.34	0.31	0.41	0.35
RNBR[d]	0.0455	0.0417	0.0345	0.0588	0.0541	0.0750	0.0333
MPPBO[e]	0.4789	0.4741	0.4803	0.8716	0.8781	0.8926	0.8614

[a] ALOGPs: Lipophilicity.
[b] ΔH_h: Hidration energy.
[c] RNAB: Relative number of aromatic bonds.
[d] RNBR: Relative number of benzene rings.
[e] MPPBO: Max pi–pi bond order.

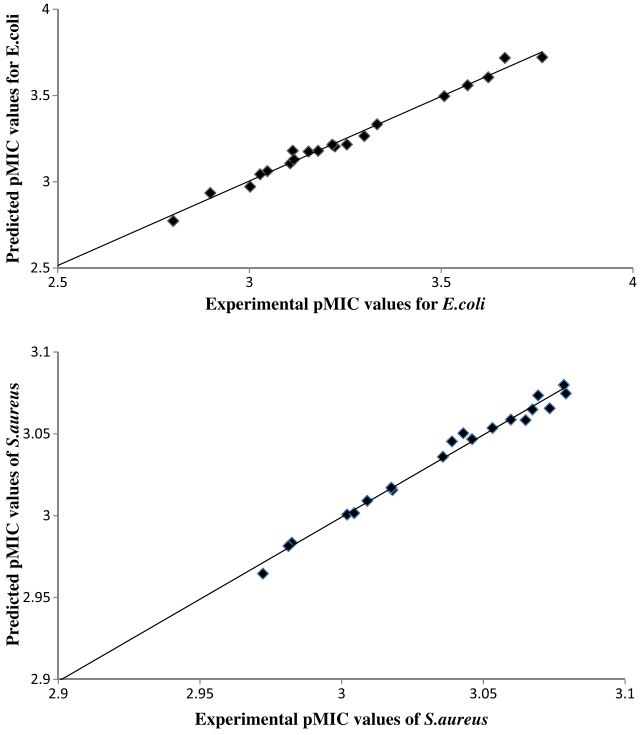

Fig. 2. Plot of experimental versus predicted pMIC values of training sets of *E. coli* and *S. aureus*.

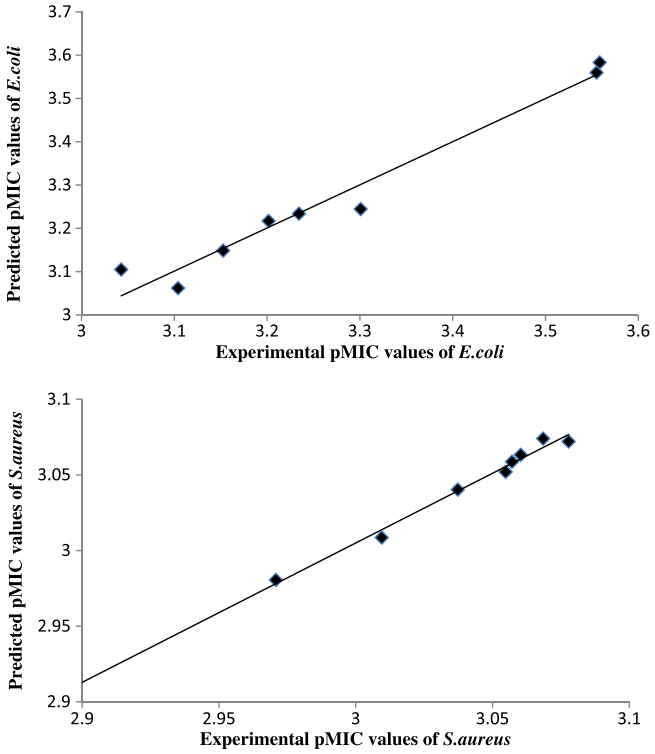

Fig. 3. Plot of experimental versus predicted pMIC values of test sets of *E. coli* and *S. aureus*.

formation and intermolecular interactions. It is known that polar interaction between molecules is directly related to the hydrogen bond or Lewis basicity of the molecule. The fourth descriptor is relative number of double bonds.

In order to confirm our QSAR equations, we have predicted the antimicrobial activity of the sulfonyl hydrazone in the test set. A graphical presentation of the relationship between the experimental and the predicted pMIC values for test sets are given in Fig. 3. Observed and predicted values are very close to each other. The test set has an acceptable external correlation coefficient ($R^2 > 0.9$).

From the model equation, we can predict that (i) point-charge on molecule affect the antimicrobial activity of the sulfonyl hydrazone (ii) presence of aromatic groups increase the antimicrobial activity (iii) sulfonyl hydrazones act as Lewis base (or nucleophile) in intermolecular interaction.

Conclusion

Obtained results demonstrate that antimicrobial activities of the sulfonamide is higher than that of corresponding sulfonyl hydrazones, and presence of OH group on sulfonamide reduces the antimicrobial activity. 2D-QSAR analysis was carried out on a series of aromatic sulfonyl hydrazones as antimicrobial agents against *E. coli* and *S. aureus*. According to the four-descriptor QSAR model, total point-charge component of the molecular dipole, HOMO energy, relative number of aromatic bonds and relative negative charged surface area play a key role in the antimicrobial activity of *E. coli*, however, partial negative surface area, maximum nucleophilic reactivity index for a N atom, H-acceptors surface area and relative number of double bonds are containing descriptors in the QSAR model for *S. aureus.* Briefly, aromatic sulfonyl hydrazones act as nucleophile in intermolecular interactions, and more aromatic bonds increase the antimicrobial activity.

Acknowledgements

The authors thank the TUBITAK (No. 104 T 390) and Gazi University BAP (No. 05/2007-01) for the financial support of this project.

References

[1] S. Rachakonda, L. Cartee, Curr. Med. Chem. 11 (2004) 775–793.
[2] C. Walsh, Antibiotics Actions Origins Resistance, ASM, Washington, DC, 2003.
[3] World Health Organisation (WHO) Geneva, World Health Report-2002, 2002.
[4] C. Nathan, Nature 431 (2004) 899.
[5] F. von Nussbaum, M. Brands, B. Hinzen, S. Weigand, D. Häbch, Angew. Chem. Int. Ed. 45 (2006) 5072.
[6] C.M. Sharaby, Spectrochim. Acta Part A 66 (2007) 1271–1278.
[7] C.M. Sharaby, G.G. Mohamed, M.M. Omar, Spectrochim. Acta Part A 66 (2007) 935–948.
[8] N.S. El-Sayed, E.R. El-Bendary, S.M. El-Ashry, M.M. El-Kerdawy Eur, J. Med. Chem. 46 (2011) 3714–3720.
[9] K.N. de Oliveira, P. Costa, J.R. Santin, L. Mazzambani, C. Burger, C. Mora, R.J. Nunes, M.M. de Souza, Bioorg. Med. Chem. 19 (2011) 4295–4306.
[10] A. Chandran, Y.S. Mary, H.T. Varghese, C.Y. Panicker, P. Pazdera, G. Rajendran, Spectrochim. Acta Part A 79 (2011) 1584–1592.
[11] M. Karabacak, E. Postalcilar, M. Cinar, Spectrochim. Acta Part A 85 (2012) 261–270.
[12] H. Alyar, A. Ünal, N. Özbek, S. Alyar, N. Karacan, Spectrochim. Acta Part A <http://dx.doi.org/10.1016/j.saa.2012.01.065>.
[13] H.A. Aslan, S. Ozcan, N. Karacan, Inorg. Chem. Commun. 14 (2011) 1550–1553.
[14] N. Özbek, S. Alyar, N. Karacan, J. Mol. Struct. 938 (2009) 48–53.
[15] N. Özbek, G. Kavak, Y. Özcan, S. Ide, N. Karacan, J. Mol. Struct. 919 (2009) 154–159.
[16] N. Özbek, H. Katircioglu, N. Karacan, T. Baykal, Bioorg. Med. Chem. 15 (2007) 7494.
[17] N.I. Dodoff, U. Ozdemir, N. Karacan, M. Georgieva, S.M. Konstantinov, M.E. Stefanova, Z Nat. 54B (1999) 1553–1562.
[18] National Committee for Clinical Laboratory Standards (NCCLS), Methods for Dilution Antimicrobial Susceptibility Tests for Bacteria that Grow Aerobically, fifth ed. Approved Standards, M7-A5. NCCLS, Wayne, PA, 2000.
[19] National Committee for Clinical Laboratory Standards (NCCLS), Performance Standards for Antimicrobial Disk Susceptibility Tests, seventh ed. Approved Standards, M2-A7. NCCLS, Wayne, PA, 2000.
[20] A.W. Bauer, W.M.M. Kirby, J.V. Sheris, M. Truck, Am. J. Clin. Pathol. 45 (1966) 493–496.
[21] S. Alyar, U.O. Ozmen, N. Karacan, J. Mol. Struct. 889 (2008) 144–149.
[22] A. Ienco, C. Mealli, P. Paoli, N.I. Dodoff, Z. Kantarci, N. Karacan, New J. Chem. 23 (1999) 1253–1260.
[23] O.S. Senturk, U. Ozdemir, S. Sert, N. Karacan, F. Ugur, J. Coord. Chem. 60 (2007) 229–235.
[24] U. Ozdemir, O.S. Senturk, S. Sert, N. Karacan, F. Ugur, J. Coord. Chem. 59 (2006) 1905–1911.
[25] U. Ozdemir, N. Karacan, O.S. Senturk, S. Sert, F. Ugur, Syn. React. Inorg. Metal. 34 (2004) 1057–1067.
[26] S. Sert, O.S. Senturk, U. Ozdemir, N. Karacan, F. Ugur, J. Coord. Chem 57 (2004) 183–188.
[27] O.S. Senturk, U. Ozdemir, S. Sert, N. Karacan, Inorg. Chem Commun. 6 (2003) 926–929.
[28] U. Ozdemir, N. Karacan, O.S. Senturk, S. Sert, F. Ugur, J. Trans. Metal. Chem. 28 (2003) 443–446.
[29] U.O. Ozmen, G. Olgun, Spectrochim. Acta A 70 (2008) 641–645.
[30] U.O. Ozdemir, P. Guvenc, E. Sahin, F. Hamurcu, Inorg. Chim. Acta 362 (2009) 2613–2618.
[31] U.O. Ozdemir, F. Arslan, F. Hamurcu, Spectrochim. Acta A 75 (2010) 121–126.
[32] M.J. Frisch et al. Gaussian, Inc., Pittsburgh PA., Gaussian 03 (Revision B.04), 2003.
[33] <http://www.vcclab.org/lab/alogps/>.
[34] HyperChem 7.5 program (2002) Hypercube Inc., Toronto, Canada.
[35] M. Karelson, Molecular Descriptors in QSAR/QSPR, John Wiley & Sons., New York, 2000. pp. 143–187 221–237.
[36] A.R. Katritzky, L.M. Pacureanu, S.H. Slavov, D.A. Dobchev, D.O. Shah, M. Karelson, Comput. Chem. Eng. 33 (2009) 321–332.
[37] A. Katritsky, M. Karelson, V.S. Lobanov, R. Dennington, T. Keith, CODESSA 2.7.10., Semichem, Inc., Shawnee, KS, 2004.
[38] R.T. Hrubiec, K. Shyam, L.A. Cosby, A.C. Sartorelli, J. Med. Chem. 29 (1986) 1777–1779.
[39] A.E. Kretov, G.V. Tikhonova, Chem. Technol. Inst., Dnepropetrovsk, Zhurnal Obshchei Khimii 29 (1959) 412–415.
[40] Salo Gronowitz, The Thiophene and Its Derivatives: Pt.4, John Wiley & Sons Inc., 1991.